ACS APPLIED ENERGY MATERIALS

www.acsaem.org Article

# Role of Mixed-Cation Perovskites in Hole Conductor-Free Perovskite Solar Cells

Adva Shpatz Dayan and Lioz Etgar*

Cite This: https://doi.org/10.1021/acsaem.3c01857 Read Online

ACCESS | Metrics & More | Article Recommendations | Supporting Information

**ABSTRACT:** In perovskite solar cells, mixed-cation perovskites offer high power conversion efficiencies due to the diverse $A^+$ cations. In these cells, the perovskite is sandwiched between electron-transport and hole-transport layers (HTL). This study presents mono- and mixed-cation perovskites in HTL-free cells: monocation ($MAPbI_3$, $FAPbI_3$) and mixed cation ($MA_{0.8}FA_{0.2}PbI_3$, $FA_{0.8}MA_{0.2}PbI_3$). Surprisingly, monocation perovskites performed better than mixed-cation perovskites in HTL-free cells due to superior hole mobility and p-type behavior, while mixed-cation perovskites work better in n-i-p and p-i-n cells. These findings highlight the electronic differences for various types of perovskite, impacting the commercialization of perovskite solar cells.

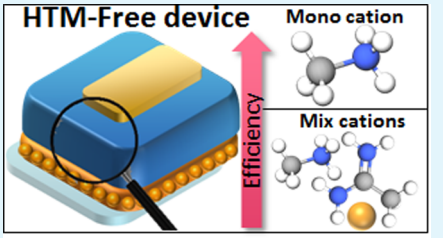


**KEYWORDS:** *hole conductor, electron conductor, perovskite, hole mobility, charge extraction*



## INTRODUCTION

The power conversion efficiency (PCE) of perovskite solar cells (PSCs) has increased rapidly in the last ten years to more than 25%, competing well with other exciting solar cell (SC) technologies.[1−3] Organic−inorganic perovskites have excellent properties such as broad absorption, long diffusion length, and a processable solution, making them suitable to function well as a light harvester in solar cells.[4]

The general formula for halide perovskites is $ABX_3$, where A is a monovalent cation ((methylammonium) $MA^+$ (formamidinium) $FA^+$, $Cs^+$), B is a divalent cation ($Pb^{2+}$, $Sn^{2+}$), and X is a halide ($I^-$, $Br^-$, and $Cl^-$).

At the beginning of the development of PSCs, the most common perovskite was $MAPbI_3$.[5] During that time, most of the research was devoted to exploring the properties of the SC while keeping the common $MAPbI_3$ perovskite. Thereafter, many reports presented the use of mixed-halide perovskite using three main halides: $I^-$, $Br^-$, and $Cl^-$. The halide mostly influences the band gap ($E_g$) of the perovskite and its stability. An additional possibility is to change the $A^+$ site cation, which also influences the optical properties but mostly the thermal properties of the perovskite.[6] To date, state-of-the-art PSCs have used perovskites with mixed cations and mixed halides.[7,8] There are two main SC structures based on perovskites: the inverted structure (p-i-n) and the n-i-p structure. In both structures, the hole-transport layer (HTL) and the electron-transport layer (ETL) are essential.

In this study, we focused on PSCs without an HTL, where the perovskite functions as a light harvester and as the HTL concomitantly. In 2012, we reported for the first time on HTL-free perovskite solar cells using $MAPbI_3$ as the light harvester and the HTL.[9] Eliminating the HTL results in a simple SC structure, reduces the cost, and avoids possible HTL degradation. When designing an HTL-free cell, two main factors must be considered. First, the energy alignment of the different layers was done in order to obtain an efficient flow of charges between the layers. Since the HTL is missing, the energy difference between the valence band of the perovskite and the work function of the metal contact is large, which creates energy loss at this interface. The second parameter that needs to be considered is the ability of the specific perovskite composition to function as an HTL and a light harvester.

There are several reports of quasi-HTL-free PSCs having different SC structures. In 2020, Danladi et al. developed HTL-free devices based on silver nanoparticles that function as the HTL, achieving a PCE of 9.05%.[10] Another example is the use of multiwalled carbon nanotubes that function as an HTL, achieving a PCE of 15.56%. Mesoscopic carbon-based PSCs[11] are also assumed to be HTL-free cells; however, the structure of this solar cell is completely different from the n-i-p or p-i-n structures and the perovskite is not sandwiched between the ETL and HTL; therefore, other layers in the solar cell function as the HTL. Moreover, in this structure, it is hard to study specifically the functionality of the perovskite as a light harvester and a hole conductor. There are a couple of reports on "classic" HTL-free perovskite solar cells having the following structure: FTO glass/mesoporous $TiO_2$/perovskite/metal contact.[12,13] Here, the perovskite's functionality

Received: July 26, 2023
Revised: October 5, 2023
Accepted: October 11, 2023

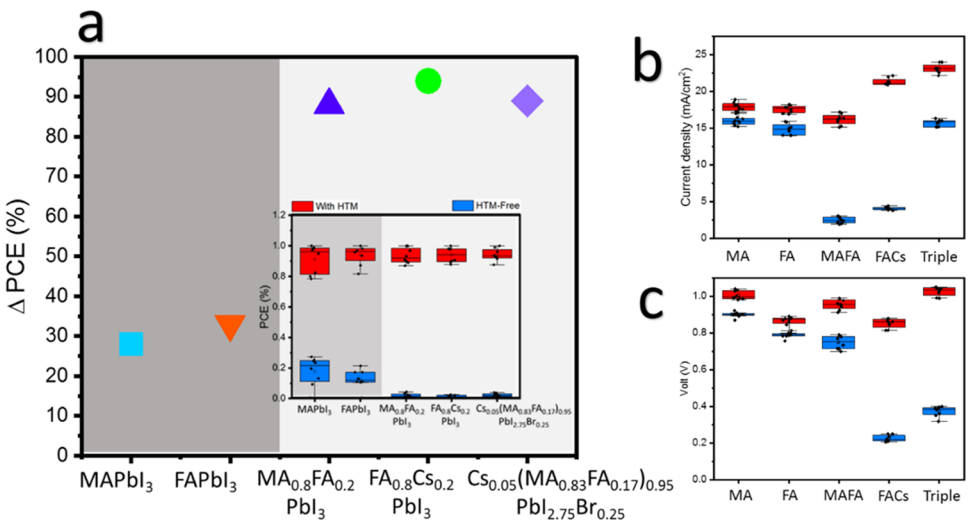


**Figure 1.** PV parameters of solar cells with and without the HTL for the five different perovskite compositions. (a) Difference in the power conversion efficiency (PCE). Inset: the absolute PCE. The difference in the PCE was calculated based on the equation: $\Delta\text{PCE}(\%) = \frac{\text{The average PCE with HTL} - \text{The average PCE without HTL}}{\text{The PCE with HTL}} \times 100\%$. (b) $J_{SC}$ and (c) $V_O$.

as a light harvester and a hole conductor is clear and can be studied.

Here, we fabricated mesoporous HTL-free PSCs using mono-, double-, and triple-mixed-cation perovskites. To the best of our knowledge, there are no reports on HTL-free solar cells (having the structure above) using a mixed-cation mixed-halide perovskite. We focused on different chemical compositions of the perovskite layer in order to study its function in HTL-free devices. In particular, we investigate the mixed-cation system and how the perovskite layer behaves in the absence of the HTL. Our hypothesis is based on the high-efficiency state-of-the-art PSCs that use mixed-cation and mixed-halide perovskites. Therefore, it can be assumed that these perovskite compositions also function efficiently in HTL-free SCs. More than that, these systems can shed more light on the perovskite's properties since we force the perovskite to work without the HTL in the solar cell.

Four different perovskite compositions, namely, $MAPbI_3$, $FAPbI_3$, $MA_{0.8}FA_{0.2}PbI_3$, and $FA_{0.8}Cs_{0.2}PbI_3$, were studied in the HTL configuration. The $A^+$ cation was changed in these compositions to determine whether it influences the perovskite's functionality when it operates in HTL-free solar cells. Currently, the reported high-efficiency perovskite in a regular mesoporous structure (with the HTL) is based on the chemical formula $Cs_{0.05}(MA_{0.83}FA_{0.17})_{0.95}PbI_{2.75}Br_{0.25}$; therefore, this composition was also evaluated in this study.[14]

## RESULTS AND DISCUSSION

Figure 1a presents the difference in the PCE for five different perovskite compositions with (red) and without (blue) the HTL. As expected, there is a difference in the PCE between cells fabricated with and without the HTL. Regarding perovskites with monocations (i.e., $MAPbI_3$ and $FAPbI_3$), there is a small drop in the PCE compared to perovskites with double and triple cations for cells with and without the HTL. With monocation perovskites, the decrease is 28 and 33% for $MAPbI_3$ and $FAPbI_3$, respectively, whereas with the double-cation perovskite, the decrease is 88 and 94% for $MA_{0.8}FA_{0.2}PbI_3$ and $FA_{0.8}Cs_{0.2}PbI_3$, respectively. The triple-cation perovskite showed a decrease of 89%.

Figure S1a presents the absorbance spectra for the four perovskite compositions. As expected, $FAPbI_3$ is red-shifted with an onset at ~810 nm, whereas $MAPbI_3$ is the most blue-shifted with an onset at ~750 nm. Similar behavior is also observed from the photoluminescence (PL) spectra (Figure S1b). The difference in the $J_{sc}$ and $V_{oc}$ values for SCs with and without the HTL is presented in Figure 1b,1c, respectively. The monocation-based cells show small differences; however, for double and triple cations, the differences are much larger. Since the band gap does not dramatically change between the various perovskites (Figure S1c), it cannot explain the difference in the $J_{sc}$ and $V_{oc}$ values; therefore, it is clear that once more than one cation is added to the perovskite composition, its ability to function in HTL-free cells decreases drastically. Figure S3 presents the MPPT tracking of the mono- and double cations. It can be seen that for the monocation compositions (MA and FA), there is a slight drop of the PCE around 20 min of the MPPT tracking, where after that, the cells are stable (Figure S3a,b). In the case of the double cations compositions, the cells are stable during the whole MPPT tracking (1 h), as shown in Figure S3c,d. It can be concluded that the direct contact of the evaporated metal with the perovskite does not harm the MPPT stability. In addition, in order to have a more general conclusion not related to a specific solar cell structure, we fabricated inverted perovskite cells with and without the HTL. $MAPbI_3$ and $Cs_{0.05}(MA_{0.83}FA_{0.17})_{0.95}I_{2.75}Br_{0.25}$ perovskites were chosen due to their better results in the HTL-free configuration. Figure S2 presents the PV parameters and JV curves for these cells. Also, in this solar cell architecture, the HTL-free cells were lower in performance in the case of the triple cation compared to the HTL-free cells in the case of the monocation.

The dark current measurements of the different compositions can be observed in Figure S4. As expected, the triple-cation cell (with the HTL) has the smallest leakage current, whereas the highest leakage current is observed in the double-cation HTL-free cells. Interestingly, the leakage currents for HTL-free and HTL cells in the case of monocations are very similar, whereas this is not the case for double and triple-cation perovskites.


https://doi.org/10.1021/acsaem.3c01857
ACS Appl. Energy Mater. XXXX, XXX, XXX−XXX

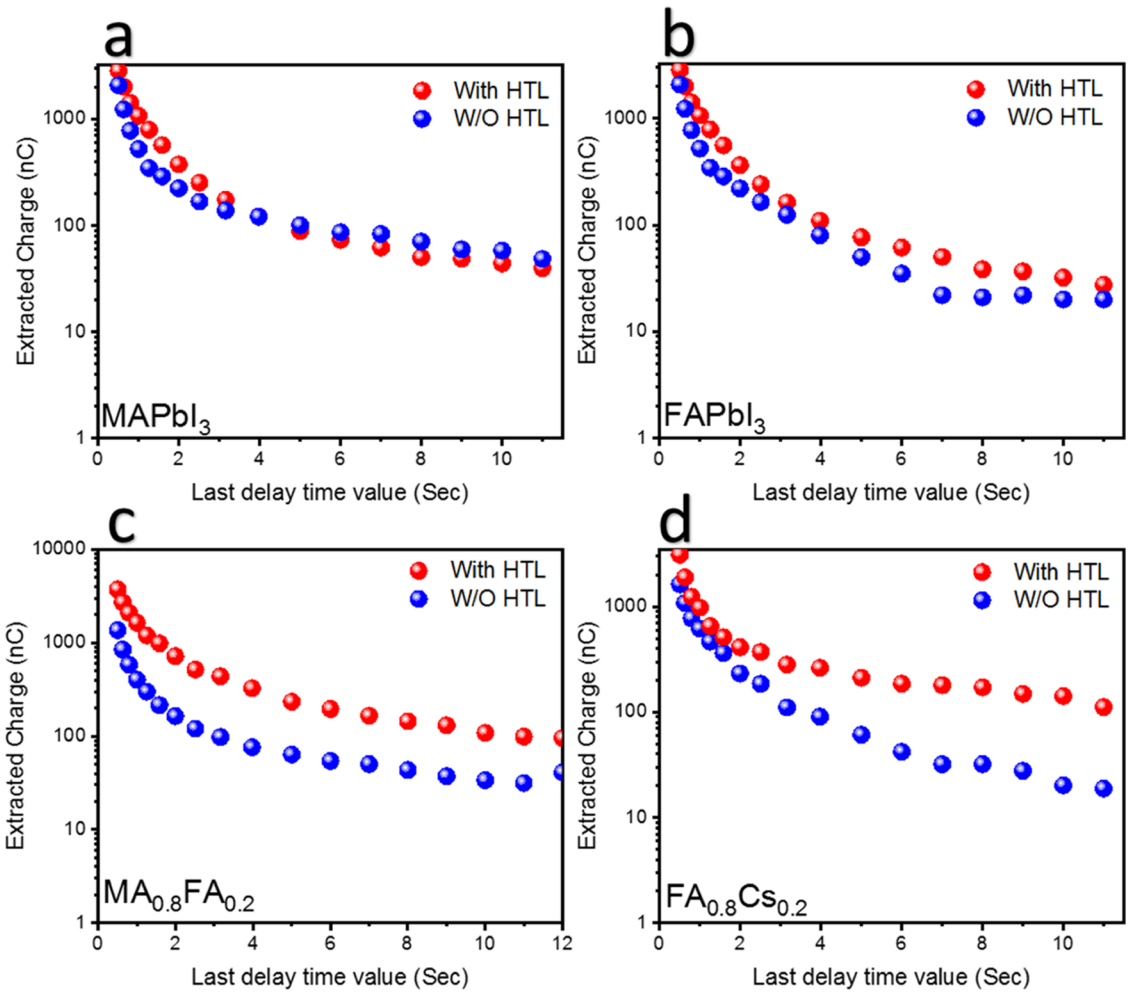


**Figure 2.** CE measurements for different perovskite compositions. The measurements are performed on a complete solar cell: (a) $MAPbI_3$, (b) $FAPbI_3$, (c) $MA_{0.8}FA_{0.2}PbI_3$, and (d) $FA_{0.8}Cs_{0.2}PbI_3$.

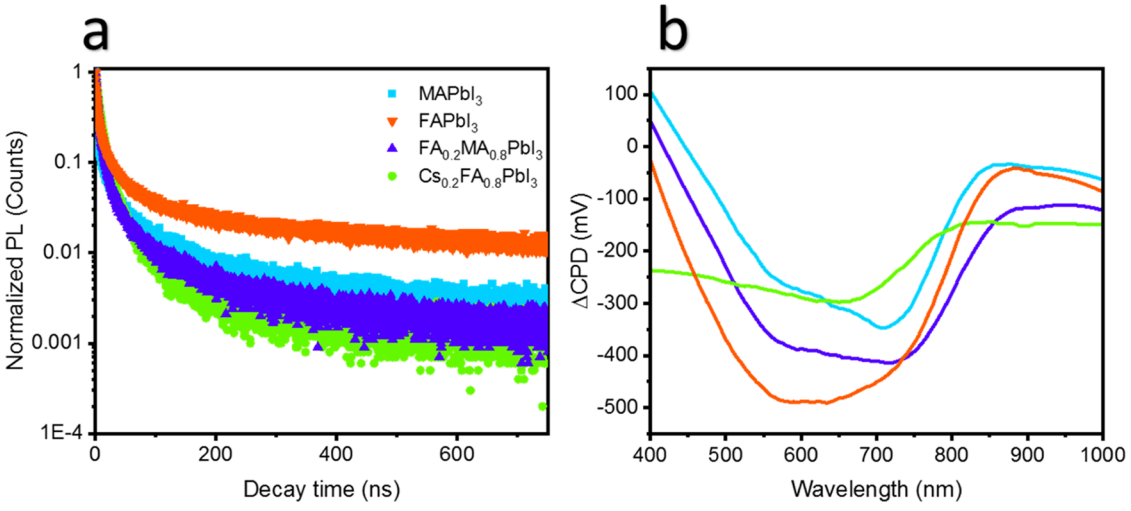


**Figure 3.** (a) PL lifetime for the five different perovskite compositions. (b) SPV spectra for the four perovskite compositions.

In order to further support the observation that adding more than one cation to the perovskite composition affects its ability to function in HTL-free cells, we performed charge extraction (CE) measurements. This analysis provides information about the transport, trapping, and back reaction of the charge carriers in the device. The charge extraction measurement consists of several steps: (i) A two s step in which the cell is discharged in the dark. (ii) The cell is then disconnected and illuminated for two s (illumination time). (iii) The light is then switched off, and the system waits a certain time (the delay time). In this step, a charge recombination occurs inside the device. (iv) The device is reconnected, and the charges that were left and did


https://doi.org/10.1021/acsaem.3c01857
ACS Appl. Energy Mater. XXXX, XXX, XXX−XXX

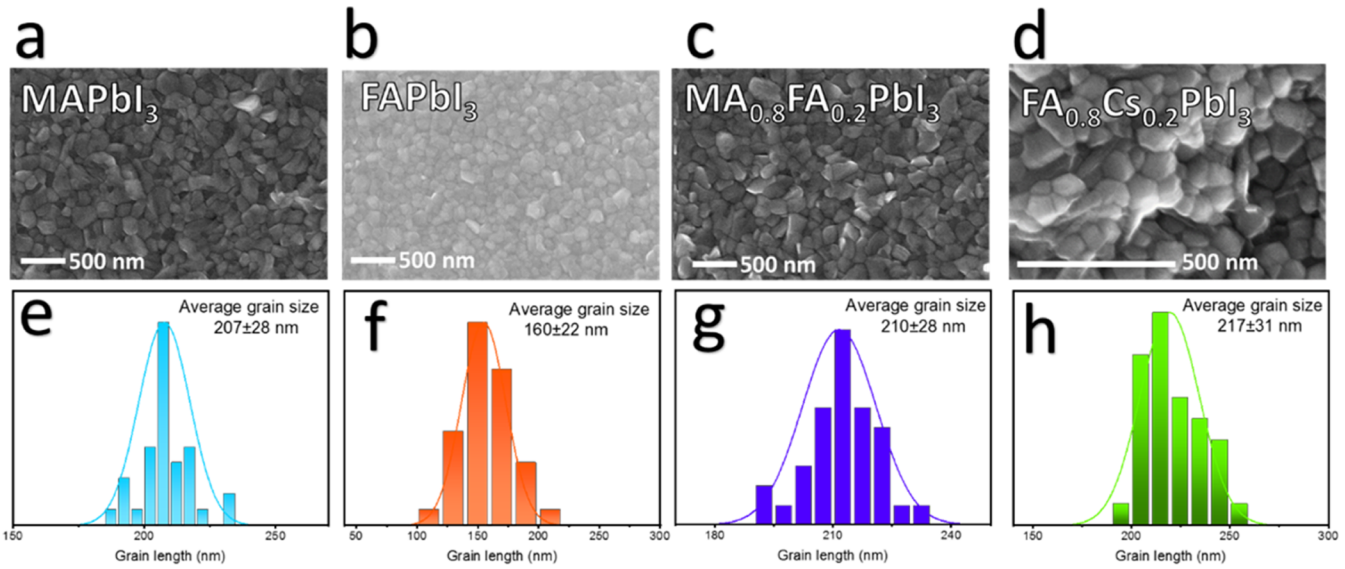


**Figure 4.** SEM micrographs for (a) $MAPbI_3$, (b) $FAPbI_3$, (c) $MA_{0.8}FA_{0.2}PbI_3$, and (d) $FA_{0.8}Cs_{0.2}PbI_3$, and the grain size distribution histogram determined from the SEM images for (e) $MAPbI_3$, (f) $FAPbI_3$, (g) $MA_{0.8}FA_{0.2}PbI_3$, and (h) $FA_{0.8}Cs_{0.2}PbI_3$.

not recombine are extracted and measured. This experiment is repeated for different delay times, ranging from 0.5 to 15 s. The accumulated charges are plotted against the delay time to provide insight into the lifetime of the charges inside the solar cell after a certain delay time. The CE analysis can be observed in Figure 2. The results show a difference for cells with monocation perovskites compared to double- or triple-cation perovskites. When the HTL is removed, there is direct contact between the perovskite and metal, which inhibits the charge extraction at this interface. However, the CE results show a difference regarding the monocation-based perovskite and the mixed-cation perovskite, even though in both cases, the perovskite is in direct contact with the metal contact. Regarding the monocation, the difference between cells with and without the HTL is small (Figure 2a,2b). While with the double and triple cations (Figures 2c,2d and S5), the difference is much larger. The small difference in the monocation indicates that the interface of $MAPbI_3/FAPbI_3$ with the metal contact does not dramatically inhibit charge extraction. However, with the mixed cation, eliminating the HTL indicates that fewer charges are left to be extracted for a certain delay time, which suggests that the rate of recombination is much faster in these cells. As discussed previously, the CE analysis further supports our observation that the mixed-cation perovskite has difficulty functioning without the HTL in the SC.

Additionally, the time-resolved PL (TRPL) was measured for different perovskite compositions (Figure 3a). In all cases, a biexponential decay curve ($y = y_0 + A_1e^{-x/\tau_1} + A_2e^{-x/\tau_2}$) was used for the fitting, where $\tau_1$ is the short PL lifetime and $\tau_2$ is the long PL lifetime. Based on several reports, it is accepted to attribute $\tau_1$ to nonradiative recombination, which usually originates from trap states and surface defects, while $\tau_2$ is associated with intrinsic radiative recombination and bulk properties.[15,16] In all the perovskite compositions, the value $\tau_2$ is larger than $\tau_1$, which indicates that the defects in the bulk are pronounced, a common phenomenon in hybrid perovskites (Table S1).[17]

External quantum efficiency (EQE) measurements can indicate three parameters: the charge collection efficiency ($\eta_c$), the charge injection efficiency ($\eta_i$), and the light-harvesting efficiency ($\eta_{lh}$). The $\eta_c$ value is affected mainly by the width of the depletion region. The depletion region parameters may vary with the voltage (and doping), which can reduce the charge collection efficiency, creating a shunting effect.[18] The value $\eta_i$ is associated with the energy levels of the complete device and specifically with the ETL and HTL.[1] For example, Jiang et al. reported that for $MAPbI_3$, the electron injection time is longer than the thermalizing process.[19] The value of $\eta_{lh}$ is influenced by the light-harvesting material in the device; here, it is related to the four compositions of the perovskite. In this work, all the layers in the SC except the light-harvesting material were kept the same. Therefore, the onset of the EQE spectra corresponds to the perovskite composition (Figure S6). This is in agreement with the absorbance spectra, as shown in Figure S1a. The main difference in the EQE for the HTL cells and the HTL-free cells is apparent in 620−800 nm wavelengths. In this region, there is a large decrease in the EQE spectra in all cases, which is related to the elimination of the HTL and associated with the charge injection efficiency ($\eta_i$).[4] Additionally, the integrated $J_{sc}$ values are in good agreement with the $J_{sc}$ measured from the solar simulator (Table S2 and Figure S7).

In order to understand why the $A^+$ cation in the perovskite structure has such a major influence on its ability to function in HTL-free SCs, we first investigated the morphology of the perovskite film. Figure 4 presents scanning electron microscopy (SEM) micrographs and histograms of the grain sizes of the four compositions. All of the perovskite compositions were deposited on $TiO_2$. It is known that when the grain size is large and there are fewer pinholes, the layer should function better in the SC.[20] The SEM micrographs present relatively similar grain sizes for all of the perovskite compositions: the highest average grain size is 217 nm for the FAC sample, and the lowest average grain size is 160 nm for the FA sample. In addition, there is no significant change in the film's pinholes between the perovskite compositions. Therefore, it is reasonable to assume that the perovskite morphology is not responsible for the difference in the PV performance for cells with and without the HTL. For example, the triple-cation


https://doi.org/10.1021/acsaem.3c01857
ACS Appl. Energy Mater. XXXX, XXX, XXX−XXX

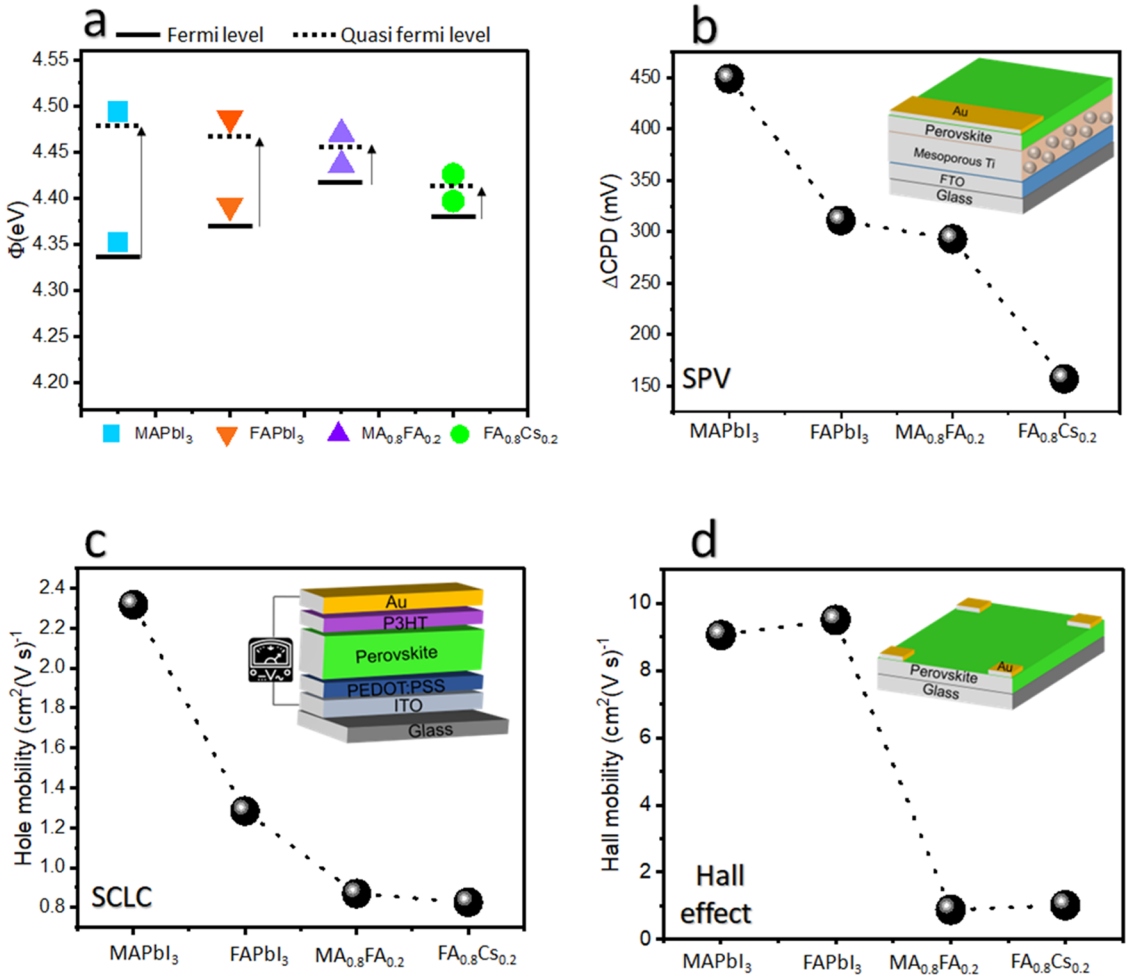


**Figure 5.** (a) Fermi level and quasi-Fermi level for the four perovskite compositions. (b) ΔCPD values for the four compositions extracted from SPV measurements (the spectra are shown in Figure 3b). (c) Hall mobility for the four compositions extracted from the space charge limited current (SCLC) measurements. (d) Hole mobility for the four compositions extracted from the Hall effect measurements.

perovskite delivers 2.4% efficiency (without the HTL) where its grain size is (217 ± 31 nm), while the MA-based perovskite demonstrates higher efficiency with a smaller grain size of 207 ± 28 nm.

When the SC is fabricated without an HTL, there is direct contact between the perovskite layer and the metal contact (Au). Therefore, the roughness of the perovskite plays a role in SC performance. For example, if the gold contact directly touches the ETL ($TiO_2$) layer, then we will observe more channels for recombination. Moreover, since Au is around 70 nm in thickness, if the roughness of the perovskite layer is higher than that, we should observe some disconductivity in the Au film. Therefore, we must ensure that the perovskite layer is pinhole-free and uniform. Cross-section SEM images show that the perovskite layer is thick and uniform (Figure S8). In order to determine the roughness of the perovskite layer, we created an atomic force microscopy (AFM) topographic image. Similar roughness was observed for all of the compositions when the smoothest perovskite is $MA_{0.8}FA_{0.2}PbI_3$ ($R_q$ = 9.5 ± 1.1 nm) and the roughest perovskite is $FA_{0.8}Cs_{0.2}PbI_3$ (($R_q$ = 24.6 ± 3.2 nm)) (Figure S9).

As discussed previously, the morphology and grain size are not the main reasons for the difference in the PV performance between mono-, double-, and triple-cation perovskites in HTL-free cells. Therefore, more physical and electrical measurements were performed.

Surface photovoltage (SPV) measurements can provide information on the Fermi and quasi-Fermi level positions in semiconductors. Figure 5a presents the SPV measured under dark and light conditions for the different perovskite compositions used in this study. The measurement under dark conditions provides the Fermi level position, whereas the measurement under light conditions indicates the quasi-Fermi level position; therefore, the difference can indicate the semiconductor type. Based on this and Figure 3b, all of the perovskites show p-type behavior. However, there is a difference in the shift of the Fermi level position between dark and light conditions for the various perovskites. If the shift between the two levels is big, the composition will be more p-type semiconductor.[21] In our measurement, it was noted that the largest difference is for the MA and then the FA monocation-based perovskite. The perovskites that show more intrinsic behavior (less p-type) are the double-cation perovskites, i.e., MAFA and CsFA. Figure 5b shows the contact potential difference (ΔCPD) measured by the SPV of the four perovskite compositions. The ΔCPD value was extracted from the SPV measurement, as shown in Figure 3b. Similar to the observation from the measurement in Figure 5a, as the ΔCPD value becomes larger, the material behavior becomes more p-


https://doi.org/10.1021/acsaem.3c01857
ACS Appl. Energy Mater. XXXX, XXX, XXX−XXX

type. It can be seen that the largest value of the ΔCPD was measured for MA-based perovskites (~450 mV), whereas the lowest value was measured for the FACs (~150 mV). These SPV measurements indicate that the electronic properties of these perovskites differ. The monocation perovskite shows distinct p-type behavior, whereas the mixed cation's composition results in a more intrinsic behavior. This observation is one explanation for the different performances of the HTL-free cells that have perovskites with mono, double, or triple cations. When the material is characterized by p-type behavior, its ability to function concomitantly as an HTL and as a light harvester is more efficient. However, if the material is characterized as being more intrinsic ("less" p-type), its ability to function concomitantly as an HTL and a light harvester is less efficient. Therefore, it appears that the mixed-cation perovskites are more efficient when they function only as light harvesters in solar cells.[22]

A common relevant technique to determine the time-averaged steady-state mobility of a semiconductor is space charge limited current (SCLC) measurement. In this method, two types of symmetric devices are fabricated: electron- and hole-only devices. In these devices, one must choose the electrodes wisely, depending on the charge that needs to be transferred (electrons or holes). Another parameter that should be taken into account is the maximum current allowed, which is defined by the buildup of the space charge. This parameter relies on the permittivity of the semiconductor; it is a product of the space charge density and charge carrier mobility. This method is well-known for working with perovskites in order to determine the trapping sites and the density of the defects.[23,23] The relationship between the voltage ($V$) and the carrier density ($J$) for SCLC is presented in the following equation $J = 9\varepsilon_0\varepsilon_r\mu_h V^2/8L^3$, while $J$ is the hole current density calculated by the space charge limited current, $\varepsilon_0$ is the permittivity of free space, $\varepsilon_r$ is the dielectric constant of the active layer, $\mu_h$ is the hole mobility, $V$ is the voltage across the device, and $L$ is the active layer thickness. The device's structure for the SCLC measurements is presented in the inset of Figure 5c. By measuring this device's structure, one can observe the curves presented in Figure S10. Using these curves and the above equation, it is possible to extract the hole mobility, as shown in Figure 5c. The MA-based perovskite exhibits the highest hole mobility of 2.3 $cm^2$ $(V\ s)^{-1}$, whereas the FACs show the lowest hole mobility of 0.87 $cm^2$ $(V\ s)^{-1}$. Several reports discuss the fact that the SCLC measurements of organic−inorganic perovskites need to be conducted with extra care due to scan-rate dependence, temperature dependence, and ion motion;[24,25] therefore, we performed additional complementary measurements (Hall effect) that can provide more information regarding the mobility of our perovskites. In this method, four metal contacts are deposited on a square sample (see the inset of Figure 5d for the device's structure). A magnetic field is applied in one direction, while an electric field is applied in a perpendicular direction, and voltage is built up across the device (called Hall voltage). Consequently, it is possible to extract the hole mobility.[26] The hole mobility is directly affected by the semiconductor type. When the Hall mobility is higher than that of other semiconductors, one can conclude that the hole conductivity is higher for this material and that it is relatively more p-type. In p-type materials, most of the majority carriers are holes. Our results show relatively the same value for $MAPbI_3$ and $FAPbI_3$ (9.06 and 9.5 $cm^2/V\ s$, respectively), whereas the mixed-cation perovskites show much lower Hall mobility values of 0.88 $cm^2/V\ s$ for MAFA and 1.02 $cm^2/V\ s$ for CsFA (Figure 5d). Both the SCLC and Hall effect measurements show the same trend regarding the Hall mobility for different perovskites. These results further support the SPV measurements, which indicate the behavior of these perovskites. As long as the perovskite is more p-type, its functionality without the HTL in the solar cell will be much more efficient. The small difference in the hole mobility values (both values are in the same order of magnitude) observed from the SLSC and Hall effect measurements is mainly due to the way in which the measurements are carried. In SCLC, the tracking is by current extraction as a function of bias voltage, which is applied to the sandwiched perovskite between two HTLs.[27] In the case of high voltage, there is a space charge limited regime, which is trap-independent and the mobility can be extracted by the Mott−Gurney law.[28] On the other hand, the Hall effect measurement method is based on an applied magnetic field perpendicular to an electric field generating a buildup voltage.[29] In this method, we change the magnetic field, and as a result, a difference between the conducting electrons and holes is observed. This results in an electrical resistivity that enables the charge carrier mobility to be extracted. An additional difference is due to the structure of the devices required for the measurements.[30] The above reasons are responsible for the deviation in the hole mobility calculation.

## CONCLUSION

In this work, we studied how the perovskite composition affects the performance of mesoporous HTL-free perovskite solar cells. The mixed-cation perovskites exhibit much lower PCE in HTL-free cells compared with the monocation perovskites. SEM and AFM measurements show similar morphologies for the mono-, double-, and triple-cation perovskites. On the other hand, SPV characterization reveals the material's p-type behavior for all compositions; however, the monocation perovskites show more p-type behavior compared with the mixed-cation perovskites. SCLC and Hall effect measurements provided us with the Hall mobilities for the different perovskites. It was found that the monocation perovskites have higher hole mobility than the mixed-cation perovskites; therefore, their functionality in HTL-free solar cells is more efficient. The mixed-cation perovskite shows an intrinsic behavior, which, on the one hand, makes them efficient as a light harvester in p-i-n or n-i-p solar cells but, on the other hand, less efficient in HTL-free solar cells. Additionally, the results were demonstrated on two kinds of solar cell architectures: the mesoporous and the inverted structures, which do not limit the conclusion of this work to a specific solar cell structure. This work discusses the different behaviors of mono- and mixed-cation perovskites in photovoltaic devices. The implication of this work is important for developing highly efficient perovskite solar cells, and it provides some future directions for the upscale of these cells.

## ASSOCIATED CONTENT

### Supporting Information

The Supporting Information is available free of charge at https://pubs.acs.org/doi/10.1021/acsaem.3c01857.

Further experimental including materials, methodologies, MPPT tracking, charge extraction, EQE, and PL lifetime (PDF)



https://doi.org/10.1021/acsaem.3c01857
ACS Appl. Energy Mater. XXXX, XXX, XXX−XXX

## AUTHOR INFORMATION


### Corresponding Author

**Lioz Etgar** − *Institute of Chemistry, Casali Center for Applied Chemistry, The Hebrew University of Jerusalem, Jerusalem 91904, Israel;* orcid.org/0000-0001-6158-8520; Email: lioz.etgar@mail.huji.ac.il

### Author

**Adva Shpatz Dayan** − *Institute of Chemistry, Casali Center for Applied Chemistry, The Hebrew University of Jerusalem, Jerusalem 91904, Israel*

Complete contact information is available at: https://pubs.acs.org/10.1021/acsaem.3c01857


### Notes

The authors declare no competing financial interest.

## ACKNOWLEDGMENTS

We would like to thank the Israel Ministry of Energy for the financial support.

## REFERENCES


(1) Alsalloum, A. Y.; Turedi, B.; Almasabi, K.; Zheng, X.; Naphade, R.; Stranks, S. D.; Mohammed, O. F.; Bakr, O. M. 22.8%-Efficient Single-Crystal Mixed-Cation Inverted Perovskite Solar Cells with a near-Optimal Bandgap. *Energy Environ. Sci.* **2021**, *14* (4), 2263−2268.

(2) NREL. Best Research-Cell Efficiency Chart | Photovoltaic Research | NREL. (accessed September 28, 2023 ) https://www.nrel.gov/pv/cell-efficiency.html.

(3) Huang, Y.; Lei, X.; He, T.; Jiang, Y.; Yuan, M. Recent Progress on Formamidinium-Dominated Perovskite Photovoltaics. *Adv. Energy Mater.* **2022**, No. 2100690.

(4) Wang, Y.; Liang, Y.; Zhang, Y.; Yang, W.; Sun, L.; Xu, D. Pushing the Envelope: Achieving an Open-Circuit Voltage of 1.18 V for Unalloyed MAPbI $_3$ Perovskite Solar Cells of a Planar Architecture. *Adv. Funct. Mater.* **2018**, *28* (30), No. 1801237.

(5) Im, J. H.; Lee, C. R.; Lee, J. W.; Park, S. W.; Park, N. G. 6.5% Efficient Perovskite Quantum-Dot-Sensitized Solar Cell. *Nanoscale* **2011**, *3* (10), 4088−4093.

(6) Jeon, N. J.; Noh, J. H.; Yang, W. S.; Kim, Y. C.; Ryu, S.; Seo, J.; Seok, S. Il. Compositional Engineering of Perovskite Materials for High-Performance Solar Cells. *Nature* **2015**, *517* (7535), 476−480.

(7) Kim, G.; Min, H.; Lee, K. S.; Lee, D. Y.; Yoon, S. M.; Seok, S. Il. Impact of Strain Relaxation on Performance of A-Formamidinium Lead Iodide Perovskite Solar Cells. *Science* **2020**, *370* (6512), 108−112.

(8) Yang, H. S.; Lee, D.; Suh, E. H.; Noh, S. H.; Lee, K. H.; Oh, J. G.; Jung, J.; Jang, J. Facile Low-Energy and Open-Air Synthesis of Mixed-Cation Perovskite Quantum Dots for High-Performance Solar Cells. *Chem. Eng. J.* **2023**, *457*, No. 141107.

(9) Etgar, L.; Gao, P.; Xue, Z.; Peng, Q.; Chandiran, A. K.; Liu, B.; Nazeeruddin, M. K.; Grätzel, M.; Gr??tzel, M. Mesoscopic CH 3NH 3PbI 3/TiO 2 Heterojunction Solar Cells. *J. Am. Chem. Soc.* **2012**, *134* (42), 17396−17399.

(10) Danladi, E.; Onimisi, M. Y.; Garba, S.; Tasiu, J. 9.05% HTM Free Perovskite Solar Cell with Negligible Hysteresis by Introducing Silver Nanoparticles Encapsulated with P4VP Polymer. *SN Appl. Sci.* **2020**, *2* (11), No. 1769.

(11) Li, S.; Li, Y.; Sun, X.; Li, Y.; Deng, F.; Tao, X. Hole Transport Layer-Free Carbon-Based Perovskite Solar Cells with High-Efficiency up to 17.49% in Air: From-Bottom-to-Top Perovskite Interface Modification. *Chem. Eng. J.* **2023**, *455*, No. 140727.

(12) Gamliel, S.; Dymshits, A.; Aharon, S.; Terkieltaub, E.; Etgar, L. Micrometer Sized Perovskite Crystals in Planar Hole Conductor Free Solar Cells. *J. Phys. Chem. C* **2015**, *119* (34), 19722−19728.

(13) Cohen, B.-E.; El; Aharon, S.; Dymshits, A.; Etgar, L. Impact of Antisolvent Treatment on Carrier Density in Efficient Hole-Conductor-Free Perovskite-Based Solar Cells. *J. Phys. Chem. C* **2016**, *120* (1), 142−147.

(14) Saliba, M.; Correa-Baena, J. P.; Wolff, C. M.; Stolterfoht, M.; Phung, N.; Albrecht, S.; Neher, D.; Abate, A. Erratum: How to Make over 20% Efficient Perovskite Solar Cells in Regular (n-i-p) and Inverted (p-i-n) Architectures. In *Chemistry of Materials*; American Chemical Society July 10, 2019; p 8576.

(15) Yang, Y.; Yan, Y.; Yang, M.; Choi, S.; Zhu, K.; Luther, J. M.; Beard, M. C. Low Surface Recombination Velocity in Solution-Grown CH 3 NH 3 PbBr 3 Perovskite Single Crystal. *Nat. Commun.* **2015**, *6* (1), No. 7961.

(16) Kara, D. A.; Cirak, D.; Gultekin, B. Decreased Surface Defects and Non-Radiative Recombination via the Passivation of the Halide Perovskite Film by 2-Thiophenecarboxylic Acid in Triple-Cation Perovskite Solar Cells. *Phys. Chem. Chem. Phys.* **2022**, *24* (17), 10384−10393.

(17) Zhang, Y.; Kim, S. G.; Lee, D.; Shin, H.; Park, N. G. Bifacial Stamping for High Efficiency Perovskite Solar Cells. *Energy Environ. Sci.* **2019**, *12* (1), 308−321.

(18) Tress, W.; Correa Baena, J. P.; Saliba, M.; Abate, A.; Graetzel, M. Inverted Current−Voltage Hysteresis in Mixed Perovskite Solar Cells: Polarization, Energy Barriers, and Defect Recombination. *Adv. Energy Mater.* **2016**, *6* (19), No. 1600396.

(19) Jiang, Y.; Juarez-Perez, E. J.; Ge, Q.; Wang, S.; Leyden, M. R.; Ono, L. K.; Raga, S. R.; Hu, J.; Qi, Y. Post-Annealing of MAPbI3 Perovskite Films with Methylamine for Efficient Perovskite Solar Cells†. *Mater. Horiz.* **2016**, *3* (6), 548−555.

(20) Dayan, A. S.; Etgar, L. Study of Electron Transport Layer-Free and Hole Transport Layer-Free Inverted Perovskite Solar Cells. *Sol. RRL* **2021**, No. 2100578.

(21) Katahara, J. K.; Hillhouse, H. W. Quasi-Fermi Level Splitting and Sub-Bandgap Absorptivity from Semiconductor Photoluminescence. *J. Appl. Phys.* **2014**, *116* (17), No. 173504.

(22) Etgar, L. Hole-Transport Material-Free Perovskite-Based Solar Cells. *MRS Bull.* **2015**, *40* (8), 674−680.

(23) Zhu, H.; Zhang, F.; Xiao, Y.; Wang, S.; Li, X. Suppressing Defects through Thiadiazole Derivatives That Modulate CH3NH3PbI3 Crystal Growth for Highly Stable Perovskite Solar Cells under Dark Conditions. *J. Mater. Chem. A* **2018**, *6* (12), 4971−4980.

(24) Sajedi Alvar, M.; Blom, P. W. M.; Wetzelaer, G. J. A. H. Space-Charge-Limited Electron and Hole Currents in Hybrid Organic-Inorganic Perovskites. *Nat. Commun.* **2020**, *11* (1), No. 4023.

(25) Le Corre, V. M.; Duijnstee, E. A.; El Tambouli, O.; Ball, J. M.; Snaith, H. J.; Lim, J.; Koster, L. J. A. Revealing Charge Carrier Mobility and Defect Densities in Metal Halide Perovskites via Space-Charge-Limited Current Measurements. *ACS Energy Lett.* **2021**, *6* (3), 1087−1094.

(26) Bernal, J. D. SEMICONDUCTING GLASSES. In *Structural Chemistry of Glasses*; Elsevier Science Ltd, 2002; pp 307−373.

(27) Saidaminov, M. I.; Abdelhady, A. L.; Murali, B.; Alarousu, E.; Burlakov, V. M.; Peng, W.; Dursun, I.; Wang, L.; He, Y.; MacUlan, G.; et al. High-Quality Bulk Hybrid Perovskite Single Crystals within Minutes by Inverse Temperature Crystallization. *Nat. Commun.* **2015**, *6* (1), No. 7586.

(28) Murgatroyd, P. N. Theory of Space-Charge-Limited Current Enhanced by Frenkel Effect. *J. Phys. D. Appl. Phys.* **1970**, *3* (2), 151−156.

(29) Mitzi, D. B.; Feild, C. A.; Schlesinger, Z.; Laibowitz, R. B. Transport, Optical, and Magnetic Properties of the Conducting Halide Perovskite Ch3nh3sni3. *J. Solid State Chem.* **1995**, *114* (1), 159−163.

(30) Stoumpos, C. C.; Malliakas, C. D.; Kanatzidis, M. G. Semiconducting Tin and Lead Iodide Perovskites with Organic Cations: Phase Transitions, High Mobilities, and near-Infrared Photoluminescent Properties. *Inorg. Chem.* **2013**, *52* (15), 9019−9038.